The transformation of an Al-based crystalline electrode material to an amorphous deposit via the electrospark welding process

S. Cadney [a], G. Goodall [a], G. Kim [b], Angela Moran [c], M. Brochu [a],*

[a] Department of Mining and Materials Engineering, McGill University, Montreal, Quebec, Canada H3A 2B2
[b] Perpetual Technologies, Canada
[c] United States Naval Academy, Annapolis, MD, USA

ARTICLE INFO

ABSTRACT

The electrospark welding process (ESW) has successfully been used to weld an aluminum-based crystalline alloy ($Al_{71.2}Co_{12.2}Ce_{16.6}$) to a zirconium-based amorphous substrate. Due to the high cooling rates involved in the ESW process, the $Al_{71.2}Co_{12.2}Ce_{16.6}$ alloy transformed into an amorphous deposit without crystallizing the substrate. This result was confirmed by X-ray diffraction. An average deposit thickness of $40 \pm 10\,\mu m$ has been obtained after 10 passes. A second series of experiments have been performed using the $Al_{71.2}Co_{12.2}Ce_{16.6}$ alloy as both the electrode and substrate material. These tests were performed to eliminate any dilution between substrate and weld deposit. Electron backscatter diffraction (EBSD) was used to verify the amorphicity of the deposit. The average weld thickness is $12 \pm 8\,\mu m$ obtained after 10 passes. It is envisioned that the process can be used for the weld repair of worn amorphous or other heat sensitive advanced materials.

© 2008 Elsevier B.V. All rights reserved.

1. Introduction

The greatest proportion of current technological advancements in the field of engineering can be attributed to the recently developed ability to produce novel materials on a large scale with diverse combinations of physical and mechanical properties [1,2]. The applications for advanced materials, such as amorphous or bulk nanomaterials, in commercial goods are increasing, however despite their improved properties, wear and surface damage continue to occur.

Weld repair can be defined as the application of material to a worn or damaged surface to obtain the original dimensions of the part [3]. The repair is normally carried out by first removing the damaged area by milling or grinding and then rebuilding the missing volume by welding with a suitable filler metal [3,4]. The physical characteristics and microstructural features inherent to metastable materials prevent traditional weld repair techniques, i.e. TIG, laser, electron beam, from being used. The large amount of heat transferred to the substrate via these processes can induce crystallization or grain growth. As a result, the successful implementation of these materials in new, demanding applications depends on the development of low cost and innovative repair techniques where the novel features of the microstructure can be maintained.

Amorphous metals or bulk metallic glasses (BMG) were discovered over 50 years ago [5], however their novel properties were never exploited in any significant industrial manner until the early 1990s when compositions with critical cooling rates (CCR) of the order of 1–100 K/s were created. Amorphous alloys are used in a wide range of applications including sporting goods, electronic casings and industrial coatings [2]. They are of particular interest due to their superior properties such as mechanical hardness and corrosion resistance in comparison to their crystalline counterparts [6]. As amorphous materials become more prevalent in commercial applications, processes capable of repairing damaged parts economically, while retaining their metastable structure will be required.

Electrospark welding (ESW) is an arc welding process that uses a short duration, high-energy electrical pulse to deposit electrode material onto a conductive substrate [7]. The apparatus consists of a rotating electrode that is connected to a high frequency power supply. As the electrode contacts the substrate material, a short circuit occurs and a deposit is created [8]. The principal advantage of the ESW process is that it is capable of creating a metallurgical bond (fused surfaces) between a deposit and a substrate while minimizing the total heat input into the material [7]. Typically, samples remain at ambient temperatures during welding and can be handled with no protection following, and even during, the process [9]. The reduction of energy input into the substrate significantly reduces any heat-affected zones (HAZ), and aids in preserving the microstructural features adjacent to the weld. The low total heat

---

* Corresponding author. Tel.: +1 514 398 2354; fax: +1 514 398 4492.
E-mail address: mathieu.brochu@mcgill.ca (M. Brochu).

input into the substrate reduces the likelihood of distortion which can be a serious concern with other, higher intensity welding processes.

Currently ESW is used for dimensional restoration of worn parts as well as applying coatings to electrically conductive materials [8]. Due to short pulse durations (4–60 μs) and high pulse frequencies (0.1–4 kHz), the ESW process is capable of dissipating heat in ~99% of the duty cycle while heating for only ~1% of that time. This results in cooling rates that may approach 10^5–10^6 °C/s [9]. The rapid cooling rates in conjunction with the very small weld volume can be sufficient to create nanostructured or amorphous deposits depending on the alloy composition and cooling rate. Also due to the low total heat input, any substrates made of thermally sensitive microstructures, i.e. bulk nanostructured or amorphous materials can be coated with this technique without destroying their novel properties. Little work has been done using the ESW process to deposit thermally sensitive materials, with few published works being the successful deposition of an iron-based amorphous alloy on stainless steel [6] and the deposition of Vitreloy 1™ on Vitreloy 1™ without inducing crystallization of neither the deposit or the substrate [10].

This paper reports the feasibility of using the ESW process as a rapid solidification process to transform an $Al_{71.2}Co_{12.2}Ce_{16.6}$ crystalline electrode material, into an amorphous deposit on both an amorphous (Vitreloy 1™) and a crystalline ($Al_{71.2}Co_{12.2}Ce_{16.6}$) substrate. A particular attention was given to study the dilution phenomenon between the filler metal and the substrate during ESW of amorphous materials.

2. Experimental procedure

A "Technocoat MicroDepo Model 150" ESW machine was used to deposit an aluminum-based crystalline alloy ($Al_{71.2}Co_{12.2}Ce_{16.6}$) onto both an amorphous substrate, commercially known as Vitreloy 1™ ($Zr_{41.2}Ti_{13.8}Ni_{10}Cu_{12.5}Be_{22.5}$), and a substrate of the same composition as the electrode to evaluate the effect of dilution in amorphous structures. The electrode material used for all experiments was $Al_{71.2}Co_{12.2}Ce_{16.6}$. The substrate was ground using SiC abrasive paper to a 600 grit finish prior to the deposition experiments. The welding was performed within a glove box purged with Ar gas to avoid oxidation. The two main parameters that were varied, capacitance and frequency, are described in Table 1. The capacitance is used as a control of the amperage within the arc, whereas the frequency relates to the number of electrical discharges or sparks per second. The rotational speed of the 2.5 mm diameter electrode was kept constant at 2500 rpm and the voltage was held fixed at 150 V throughout the experiment. The spark energy was calculated using $E = \frac{1}{2}CV^2$ [11], where C is the capacitance and V is the voltage, respectively. The deposition energy was varied between 0.9 and 1.7 J for the Vitreloy 1™/$Al_{71.2}Co_{12.2}Ce_{16.6}$ combination and between 1.1 and 1.7 J for the $Al_{71.2}Co_{12.2}Ce_{16.6}$/$Al_{71.2}Co_{12.2}Ce_{16.6}$ combination. A duty cycle was used whereby the electrode was in contact with the substrate for 10 s, then removed and allowed to cool in the Ar gas stream for 10 s. A total of 10 cycles were performed for each test. After each cycle the direction of rotation was changed to prevent any preferential topography from developing on the surface of the coatings. The deposits were produced over a region measuring approximately 1 cm by 1 cm.

X-ray diffraction analysis was carried out using a Phillips PW1070 Cu Kα diffractometer (λ = 1.54056 Å) operated at 40 kV and 20 mA was used to study the phase composition and crystallinity of the base material and the deposit after welding. For microstructural analysis, the samples were sectioned using a slow speed diamond blade, mounted in epoxy resin, ground using SiC paper and polished with diamond paste. The final polishing stage was performed using 0.05 μm colloidal silica. The microstructure was analyzed using scanning electron microscopy using a Hitachi S-4700 field emission scanning electron microscope (FESEM) equipped with an Oxford EDS detector. The microscope was operated at 10 keV and a beam current of 20 mA. The measurements on the micrographs were performed using the Clemex Image Analysis software. Electron backscatter diffraction (EBSD) was performed on
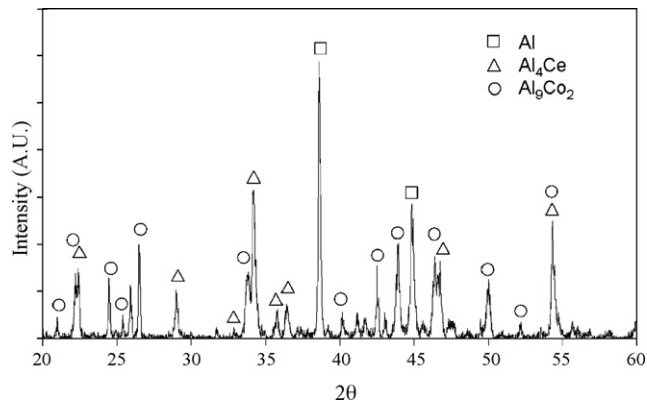

Fig. 1. XRD pattern of the crystalline $Al_{71.2}Co_{12.2}Ce_{16.6}$ alloy.

a Hitachi S3000N microscope equipped with an hkl EBSD detector, in which the sample was tilt over 70° to reveal the Kikuchi patterns.

3. Results and discussion

Section 3 will be divided into two segments. Section 3.1 will present data from the series of experiments where the $Al_{71.2}Co_{12.2}Ce_{16.6}$ crystalline alloy was welded onto an amorphous substrate. Section 3.2 will present the results from the $Al_{71.2}Co_{12.2}Ce_{16.6}$ alloy deposited on a crystalline substrate of the same composition.

3.1. Deposition of $Al_{71.2}Co_{12.2}Ce_{16.6}$ on Vitreloy 1

Fig. 1 depicts the XRD patterns of the "as received" crystalline $Al_{71.2}Co_{12.2}Ce_{16.6}$ alloy where the three primary crystallization phases, Al (JCPDS 04-0787), Al_9Co_2 (JCPDS 30-0007) and Al_4Ce (JCPDS 19-0006), are indicated. The X-ray penetration depth for the $Al_{71.2}Co_{12.2}Ce_{16.6}$ alloy has been calculated to be between 15 and 60 μm over the 2θ range scanned during the XRD experiments. Fig. 2 presents a representative back-scattering micrograph of the coating/substrate interface after a 10 pass deposit. The average coating thickness measured was 40 ± 10 μm, which results in an average thickening rate of 4 μm/pass. As can be seen, the deposit shows a low level of porosity or defects.

Fig. 3 presents two XRD patterns of tests performed where two parameters, namely capacitance and frequency, were varied as follows: 100 μF, 65 Hz and 150 μF, 150 Hz. The pattern obtained for the former set of parameters is typical of the lower heat input coatings (E = 1.1 J), whereas the pattern obtained for the latter set is representative of the higher energy input parameters (E = 1.7 J). As can be seen, the general shape of the XRD pattern is similar to that of an amorphous material. However, two crystalline peaks were observed for the low-energy deposit while four peaks were observed for the high-energy coatings. By comparing the measured deposit thickness and the X-ray penetration depth within the $Al_{71.2}Co_{12.2}Ce_{16.6}$ alloy (between 15 and 60 μm), one can deduce that the acquired signal emanates from both the deposit and the substrate. Two of the four peaks observed for the deposit performed

Table 1
Range of parameters used to successfully transform crystalline electrode material to an amorphous deposit

Substrate	Electrode	Capacitance (μF)	Frequency (Hz)	Energy (J)
Vitreloy 1™	$Al_{71.2}Co_{12.2}Ce_{16.6}$	80–150	60–150	0.9–1.7
$Al_{71.2}Co_{12.2}Ce_{16.6}$	$Al_{71.2}Co_{12.2}Ce_{16.6}$	100–150	60–90	1.1–1.7